COMPARISON BETWEEN TWO WALL TREATMENTS IN THE THREE-DIMENSIONAL MODELING OF A INTERNAL COMBUSTION ENGINE

Flavio V Zancanaro Jr, zancanaro@mecanica.ufrgs.br
Carlos E G Falcão, smkadu@yahoo.com.br
Charles Rech, charlesrech@uol.com.br
Giovanni S Andrade, giovannirs@terra.com.br
Horácio A Vielmo, vielmoh@mecanica.ufrgs.br
Mechanical Engineering Department, Federal University of Rio Grande do Sul,
Rua Sarmento Leite, 425, CEP 90050-170, Porto Alegre, RS, Brazil.

Abstract. *This paper compares the effects of the wall treatment in the three-dimensional modeling of the intake and in-cylinder systems of a Diesel engine during the intake process, under the motored condition. The engine geometry comprising a bowl-in-piston combustion chamber, intake port of shallow ramp helical type and exhaust port of conventional type. The equations are numerically solved, including a transient analysis, valves and piston movements, for engine speed of 1500 rpm, using a commercial Finite Volumes CFD code. For the purpose of examining the in-cylinder turbulence characteristics two parameters are observed: the discharge coefficient and swirl ratio. Additionally, the evolutions along crank angle of the discharge coefficient and swirl ratio are compared, with the objective of clarifying the physical mechanisms. Regarding the turbulence, computations are performed with the Eddy Viscosity Model k-ω SST, in its Low-Reynolds approaches, with hybrid and standard near wall treatments. The system of partial differential equations to be solved consists of the Reynolds-averaged compressible Navier-Stokes equations with the constitutive relations for an ideal gas, and using a segregated solution algorithm. The enthalpy equation is also solved. A moving hexahedral trimmed mesh independence study is presented. In the same way many convergence tests are performed, and a secure criterion established. Areas of low pressure can be seen in the valve curtain region, due to strong jet flows. Also, it is possible to note agreements between the wall treatments, mainly for the discharge coefficient.*

Keywords*: Diesel engine, transient analysis, CFD, moving mesh, turbulence model, wall treatments.*

1. INTRODUCTION

With the exponentially increasing computational power of modern computers, multi-dimensional Computational Fluid Dynamics (CFD) has found more and more applications in internal combustion engines (ICE) research, design and development. Enhanced understandings of the physical processes of combustion and correspondingly improved numerical models and methods have both driven multi-dimensional CFD simulation tools from qualitative description towards quantitative prediction (Lakshminarayanan and Aghav, 2010). Therefore, powerful CFD codes are required to have the capability of predicting complex turbulent flows from engine developments and design in a reasonable time scale.

In-cylinder flows of diesel engines are typically compressible turbulent flows. Turbulence by itself remains one of the most complex fundamental problems of fluid dynamics. The complexity of in-cylinder flows is further increased due to transient swirling flows, considering the usual complexity of the geometry, the large turbulence spectra associated with the annular vortical jet after the intake valve, adding the compressible non-isothermal effects. The detailed understanding of the flow dynamics characteristics of intake, cylinder and exhaust flow of ICE is necessary for an efficient combustion process and related emissions to the environment. Therefore, a numerical approach could thus be an alternative due to the capability of CFD for in-cylinder flow predictions in recent 20 years. Gosman (1985) can be regarded as one of the pioneers in the application of CFD simulation to investigate in-cylinder flows. Since then tremendous improvements have been achieved in computational techniques in this field of study.

During the last years more numerical simulations have been done regarding the discharge coefficient (Bianchi *et al.*, 2002a ; Bianchi and Fontanesi, 2003), focusing on directed intake port types, including comparisons with experimental measurements. An even more challenging situation occurs in the presence of swirl generator inlet ports of ramp helical type, including the determination of the swirl ratio. With the growing availability of turbulence models and computational resources, many works make comparisons, regarding their capacity to reproduce experimental data and CPU time demanding.

The compared *k-ε* linear and nonlinear (quadratic and cubic) eddy viscosity models (Bianchi *et al.*, 2002b) concluding that cubic stress-strain relation provided the best agreement with data, for those ICE three-dimensional flows considered. In another work, Bianchi *et al.* (2002a) investigated the High Reynolds and Low Reynolds near wall approaches, both with a cubic relationship between Reynolds stresses and strains. It was concluded that the Low

Reynolds approach (boundary layer also discretized by the mesh), although increasing the computational effort, presented more ability to capture the details of the tested ICE intake flow.

In a typical steady flow condition, Baratta *et al.* (2008) compared the *k-ε* cubic, in its High-Reynolds and Low-Reynolds approaches, for fixed intake valve lifts steady state situations. Thought the results it was possible to note significant divergences between the turbulence models employed, mainly in the calculated swirl ratio.

The present paper focuses on a transient numerical analysis of the same Diesel engine (Fiat Research Center, 1982, 1983) analyzed in Baratta *et al.* (2008, 2009). Looking for more suitable turbulence models, the *k-ω* SST, in its Low-Reynolds approach, in its compressible and non-isothermal approach, were compared, regarding mainly the discharge coefficient and swirl ratio.

2. CASE DESCRIPTION

The engine under investigation is of a four-stroke compression-ignition, direct-injection single cylinder (Fig. 1). It was derived from an automotive diesel engine at Fiat Research Center. The engine had a swirl generator inlet port of shallow ramp helical type (Fiat Research Center, 1982 ; Tindal *et al.*, 1982). It is coupled with a seat valve with an inner diameter of 31.5 mm, and outer diameter of 34.5 mm. The outlet port is a conventional one, with a valve of an inner diameter of 26.7 mm, and outer diameter of 29.5 mm. The cylinder bore is 79.5 mm, stroke 86 mm, and compression ratio 18:1. The maximum intake valve lift is 8.1 mm, opening at 355^o (5^o before TDC) and closing at 595^o (55^o after BDC). The maximum exhaust valve lift is 8.1 mm, opening at 125^o (55^o before BDC) and closing at 365^o (5^o after TDC).

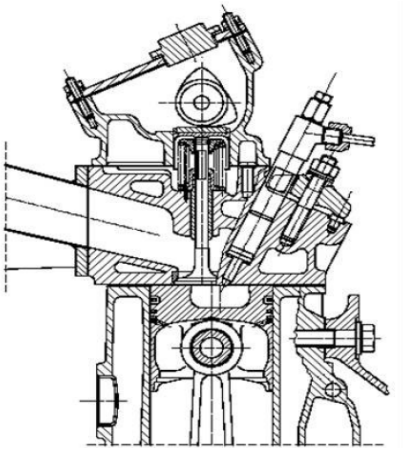

Figure 1. 1.9-L Fiat engine (Fiat Research Center, 1982; 1983)

2.1. Boundary and Initial Conditions

The boundary conditions are stagnation pressure (p_{st}) of 1 atm at the inlet, with 293.15 K, discharging in an ambient pressure (p_{out}) of 1 atm, and 293.15 K.

For all cases the turbulence boundary conditions are turbulence intensity $I = 0.05$, and length scale l = 0.0035 m, as a consequence of the flow and geometrical characteristics.

Regarding the heat transfer problem, considering a cold flow (exhaust and compression processes, without combustion), the cylinder wall and piston crown have a constant temperature of 400 K, and a thermal resistance of 0.004 m^{2}K/W. For the combustion dome 450 K and 0.004 m^{2}K/W. For the admission and exhaust valves and ports 350 K and 0.004 m^{2}K/W.

As initial condition for the independency mesh analysis, the crankshaft starts at 320º, almost at the end of the exhaust process, followed by the valve crossing, and after the air admission. All the velocity components inside the cylinder are set 1 m/s, at 1 atm and 300 K. For the rest of the simulations, the initial conditions are the final fields of the previous cycle.

3. MATHEMATICAL MODEL

3.1. Governing Equations

The velocity field is described by the mass and momentum conservation equations (Navier-Stokes), in their transient, compressible form.

In Cartesian tensor notation, according Warsi (1981), the mass conservation is

$$\frac{\partial \rho}{\partial t} + \frac{\partial}{\partial x_j}\left(\rho u_j\right) = 0 \tag{1}$$

and the momentum

$$\frac{\partial \rho u_i}{\partial t} + \frac{\partial}{\partial x_j}\left(\rho u_j u_i - \tau_{ij}\right) = -\frac{\partial p}{\partial x_i} + s_i \tag{2}$$

where

$$p = p_s - \rho_0 g_m x_m \tag{3}$$

As the fluid is Newtonian, and the flow is turbulent, assuming the ensemble average (equivalent to time averages for steady-state situations), the stress tensor components are, according Hinze (1975),

$$\tau_{ij} = 2\mu S_{ij} - \frac{2}{3}\mu \frac{\partial u_k}{\partial x_k}\delta_{ij} - \overline{\rho u_i' u_j'} \tag{4}$$

and strain tensor

$$S_{ij} = \frac{1}{2}\left(\frac{\partial u_i}{\partial x_j} + \frac{\partial u_j}{\partial x_i}\right) \tag{5}$$

The u' are fluctuations about the ensemble average velocity, and overbar denotes the ensemble averaging process. Finally, as the flow is compressible and non-isothermal

$$s_i = g_i(\rho - \rho_0) \tag{6}$$

where g_i is the gravitational acceleration component in x_i direction. Considering the air as an ideal gas

$$\rho = \frac{p}{RT} \tag{7}$$

For the heat transfer problem, the enthalpy equation is also solved. According Jones (1980),

$$\frac{\partial \rho h}{\partial t} + \frac{\partial}{\partial x_j}\left(\rho h u_j + F_{h,j}\right) = \frac{\partial p}{\partial t} + u_j \frac{\partial p}{\partial x_j} + \tau_{ij}\frac{\partial u_i}{\partial x_j} \tag{8}$$

where $h = \overline{c}_p T - c_p^0 T_0$ is the static enthalpy; $\overline{c}_p$ is the mean constant-pressure specific heat at temperature T; c_p^0 the reference specific heat at temperature T_0, and $F_{h,j}$ the diffusional energy flux in direction x_j, given by

$$F_{h,j} \equiv -k_t \frac{\partial T}{\partial x_j} + \overline{\rho u_i' h'} \tag{9}$$

where k_t is the thermal conductivity.

3.2. Governing Equations for the SST *k-ω* Model

The specific dissipation rate is defined as $\omega = \varepsilon / C_\mu k$, and the general form of the turbulent kinetic energy is

$$\frac{\partial}{\partial t}(\rho k) + \frac{\partial}{\partial x_j}\left[\rho u_j k - \left(\mu + \frac{\mu_t}{\sigma_k^\omega}\right)\frac{\partial k}{\partial x_j}\right] = \mu_t P - \rho\beta^* k\omega + \mu_t P_B \tag{10}$$

and specific dissipation rate is

$$\frac{\partial}{\partial t}(\rho\omega) + \frac{\partial}{\partial x_j}\left[\rho u_j \omega - \left(\mu + \frac{\mu_t}{\sigma_\omega^\omega}\right)\frac{\partial \omega}{\partial x_j}\right] = \alpha\frac{\omega}{k}\mu_t P - \rho\beta\omega^2 + \rho S_\omega + C_{\varepsilon 3}\mu_t P_B C_\mu \omega \tag{11}$$

where

$$P \equiv S_{ij} \frac{\partial u_i}{\partial x_j} \quad ; \quad P_B \equiv -\frac{g_i}{\sigma_{h,t}} \frac{1}{\rho} \frac{\partial \rho}{\partial x_i} \tag{12}$$

where $C_{\varepsilon 3}$ and C_μ are empirical coefficients. For k-ω SST model, the other coefficients are given in Menter (1993). In the SST k-ω model the turbulent viscosity is linked to k and ω via

$$\mu_t = \frac{a_1 k}{\max\left(a_1 \omega, \sqrt{\frac{1}{2}\Omega_{ij}\Omega_{ij}} \; F_2 \right)} \tag{13}$$

4. NUMERICAL METHODOLOGY

Numerical transient solutions using a commercial Finite Volumes CFD code (Star-cd, 2008) were performed, for an engine speed (N) of 1500 rpm. A user defined unstructured hexahedral-trimmed cells moving mesh was constructed, as showed in the Fig. 2. A mesh independence study was performed, arriving in 1057084 cells in the cylinder, 352976 in the inlet port and 261996 in the exhaust port.

For the turbulence models applied, k-ω SST, in its Low-Reynolds approach, with hybrid and standard near wall treatments. All computations were performed in double precision. The pressure-velocity coupling is solved thought the SIMPLE algorithm.

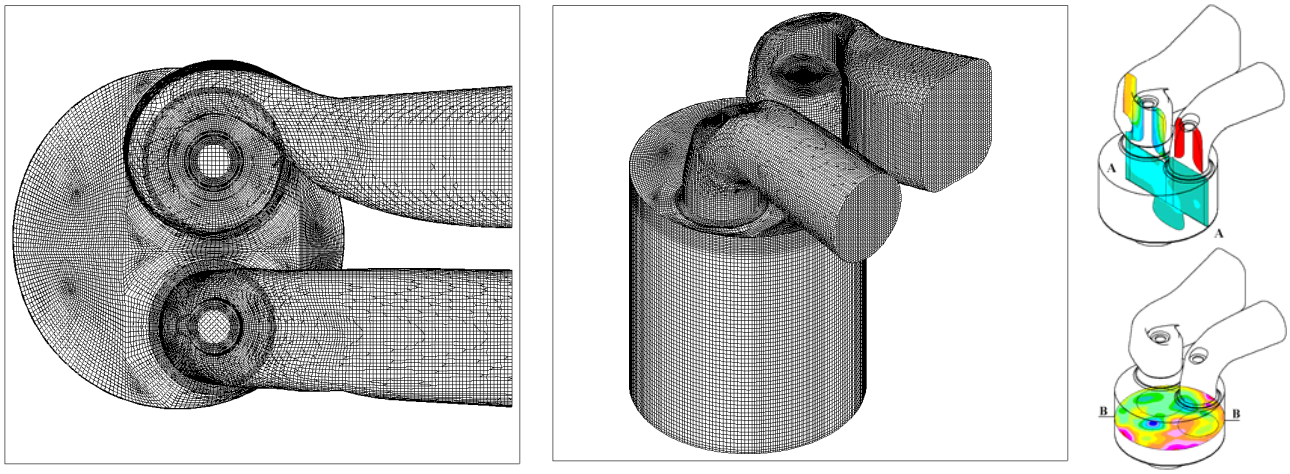

Figure 2. Unstructured hexahedral-trimmed cells moving mesh

By the complexity of the flow, aiming a stable solution, it was necessary to underrelax the momentum with 0.4, pressure 0.2, temperature 0.6, k-ε-ω 0.6, density 0.4, viscosity 0.4.

The time integration was made thought a fully implicit Euler scheme, with a constant time step of 5.5555E-6 s (0.05º), for a crank angular velocity of 1500 rpm.

The linear algebraic equations system was solved by the method of scalar preconditioned conjugate gradient.

As differencing schemes, were applied the Linear Upwind Differencing (LUD), according Wilkes and Thompson (1983), with blending factor (bf) of 0.3 for the momentum, turbulence and enthalpy equations. For the density the Central Differencing (CD) with bf = 0.3 (Hirsch, 2007).

5. THE DISCHARGE COEFFICIENT AND SWIRL RATIO

5.1. Discharge Coefficient

The discharge coefficient is a relation between the ideal and real air mass flow rate, that obtained in an isentropic expansion through the area $\pi d^2/4$. Therefore, the equation assumes the following form (Heywood, 1988 ; Ferrari, 2005),

$$C_D = \frac{\dot{m}_{actual}}{\dot{m}_{ideal}} = \frac{\dot{m}_{actual}}{\frac{\pi d^2}{4}\frac{p_{st}}{(RT_0)^{1/2}}\left(\frac{p_{out}}{p_{st}}\right)^{1/\gamma}\left\{\frac{2\gamma}{\gamma-1}\left[1-\left(\frac{p_{out}}{p_{st}}\right)^{(\gamma-1)/\gamma}\right]\right\}^{1/2}} \tag{14}$$

where $\dot{m}_{actual}$ is obtained experimentally or numerically, d is the inner valve diameter, R is the universal gas constant, γ is the specific heat ratio and T is the temperature.

5.2. Swirl Ratio

The swirl ratio, R_s, is a normalized value used to show the motion pattern of the rotating fluid within the cylinder. Assuming that flow inside the cylinder is a solid body rotational flow, the swirl ratio is obtained by dividing the rotational angular velocity (ω_s) by the crankshaft rotational velocity, as follows (Heywood, 1988)

$$R_s = \frac{\omega_s}{(2\pi N)/60} \tag{15}$$

The direction of swirl ratio is determined according to the right-hand rule. The swirl center can be the cylinder axis or the center of mass. For this case, the center of mass is not located on the cylinder axis, because the piston bowl is not centrally localized. Following the Star-cd (2008), the swirl ratio is computed on the basics of the total angular momentum relative to the center of mass along the cylinder axis, and the engine speed.

Then, the swirl ratio is computed as

$$R_S = \frac{\sum_{cells}\rho_i V_i\left[(x_i - x_m)v_i - (y_i - y_m)u_i\right]}{2\pi\frac{N}{60}I_z} \tag{16}$$

where x_i, y_i and z_i are the centroid coordinates of cell i, x_m, y_m and z_m are the center of mass coordinates, w_i and v_i are velocity components, ρ_i is the density, V_i is the volume of cell i and I_z is the moment of inertia, which can be computed as follows

$$I_z = \sum_{cells}\rho_i V_i\left((y_i - y_m)^2 + (x_i - x_m)^2\right) \tag{17}$$

6. RESULTS AND DISCUSSION

The correct evaluation of near-wall effects represents a critical objective, especially when considering ICE flows, because of both the presence of separated flows and the considerable variations of the Reynolds number throughout the computational domain. The different situations in domain become a challenging the task of mesh generation and the choice of appropriate wall treatment. The Low-Reynolds modeling, using standard wall treatment, requires a very fine grids in wall regions, with y^+ of the order of 1. By the other way, the hybrid wall treatment gives more flexibility, with $0.1 < y^+ < 100$ (Star-cd, 2009).

In order to compare the results produced by the two wall treatments (hybrid and standard), the following figures show velocity vectors and pressure fields for a crank angle of 74° after TDC, close to the maximum piston velocity, where it can be verified the extreme situations, regarding the flow complexity. The time period, since the initial condition, is 0.0926667 s, corresponding to an angular interval of 834º (320º – 1154º). The intake valve lift in this moment is 6.839 mm.

Two significant sections are showed, being important to point that the unique difference between these solutions is the wall treatment (same boundary and initial conditions, mesh, time step, differencing schemes, turbulence model, etc.).

The Figure 3 illustrates the behavior of the y^+ on the computational domain at 1154º. It possible to note that on intake steam valve shows an increase in y^+, due to high velocities to impinge with the valve. This behavior is not desired for the standard wall treatment, but for hybrid wall treatment the commitment is the responsibility of the hybrid method, showing to be a good alternative to this situation.

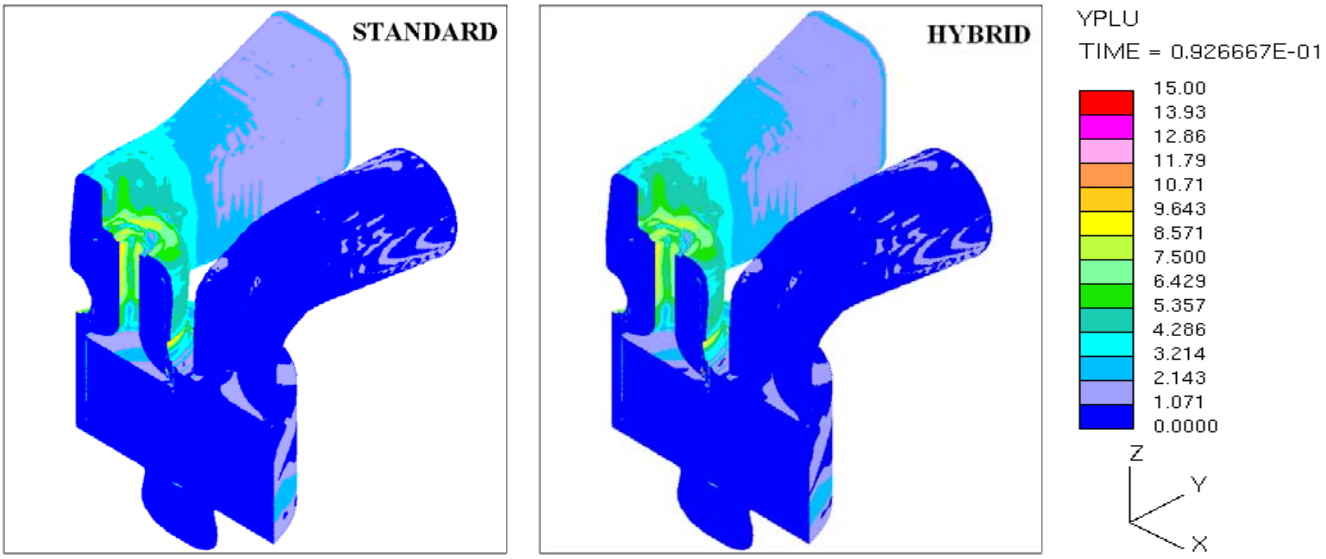

Figure 3. y^+, at 1154º

The Figure 4 shows that the flow patterns produced by each wall treatments are similar. It can also be seen that the annular vortical jets caused by the valve have different dimensions and peak velocities (108.5 m/s for the standard wall treatment and 109.3 m/s for the hybrid wall treatment). The local recirculation at the end of the valve rod – beginning of the valve plane, already detected in previous works Baratta *et al.* (2008), is also present.

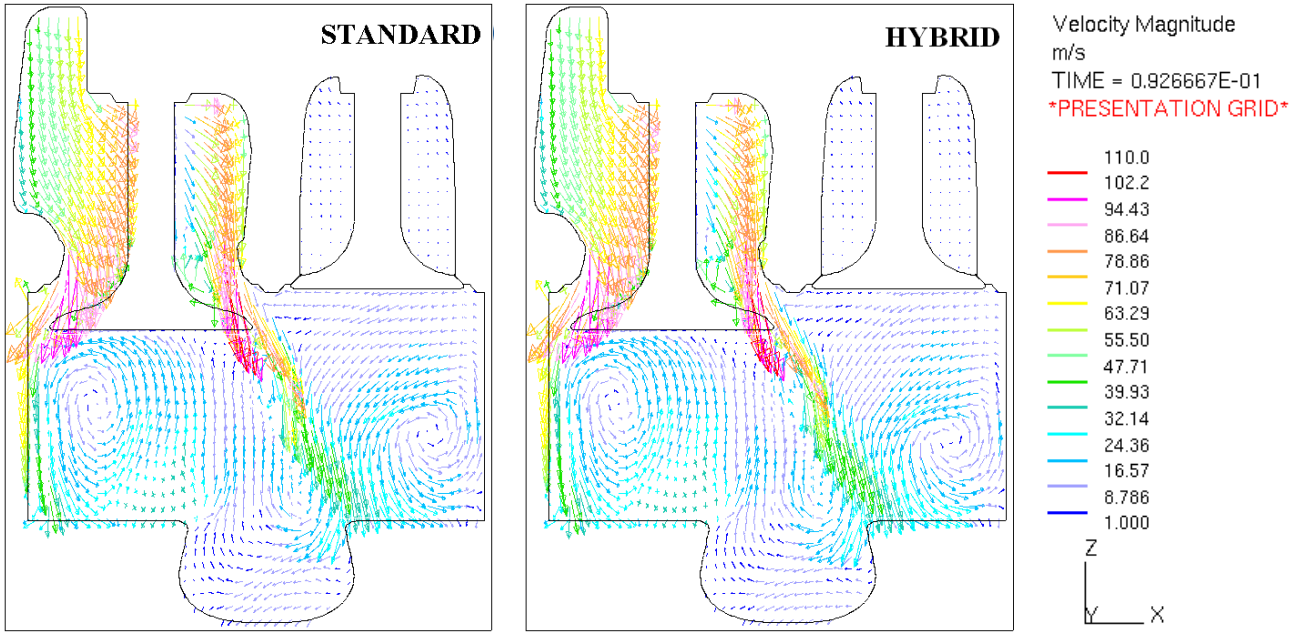

Figure 4. Velocity vectors on section A-A, at 1154º

In the Figure 5, it is possible to observe the complexity of the flow, with counterclockwise and clockwise vortices, with different intensities. Also, there is a variation in the vortices shapes, as well as the position of their centers. The point of maximum velocity occurs near the cylinder wall; 61.79 m/s for the standard wall treatment and 61.15 m/s for the hybrid wall treatment.

Focusing the pressure fields, the Figure 6 shows, as expected, the minimum values near the valve seat (maximum velocities). After this region, the pressure returns increasing to cylinder inside, according the decrease of velocities.

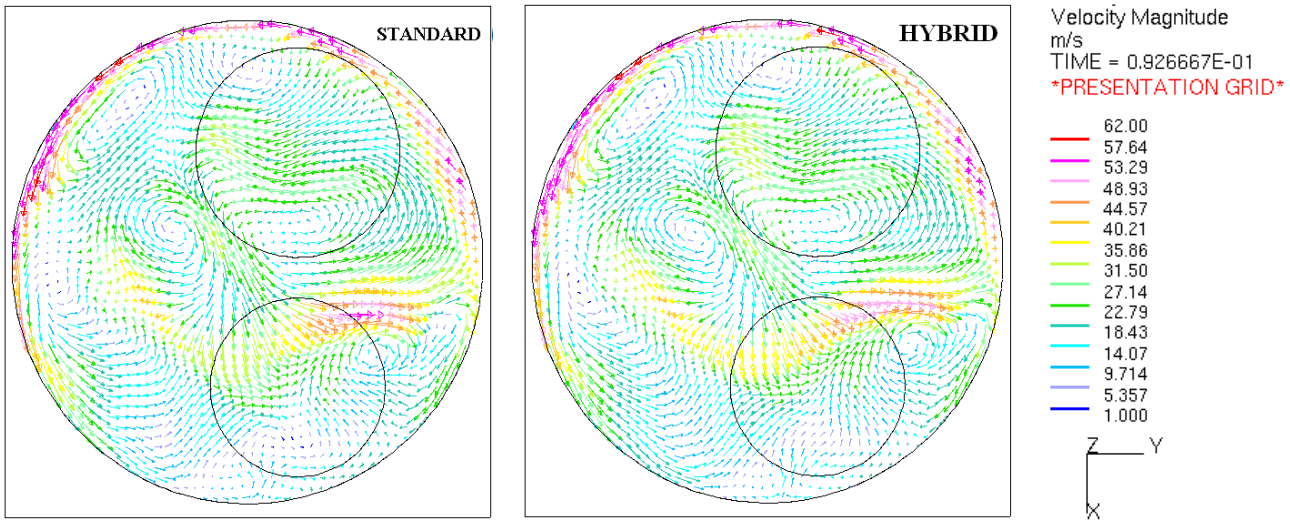

Figure 5. Velocity vectors on section B-B, at 1154°

The minimum absolute pressure at A-A cut is 91.46 kPa, for the standard wall treatment, and 91.35 kPa for the hybrid wall treatment. These differences can be noted in the figures more clearly than in the vector fields.

As already seen for the pressure fields, it is possible to see in the Figure 7 a little variation between the wall treatments, when examining the section B-B.

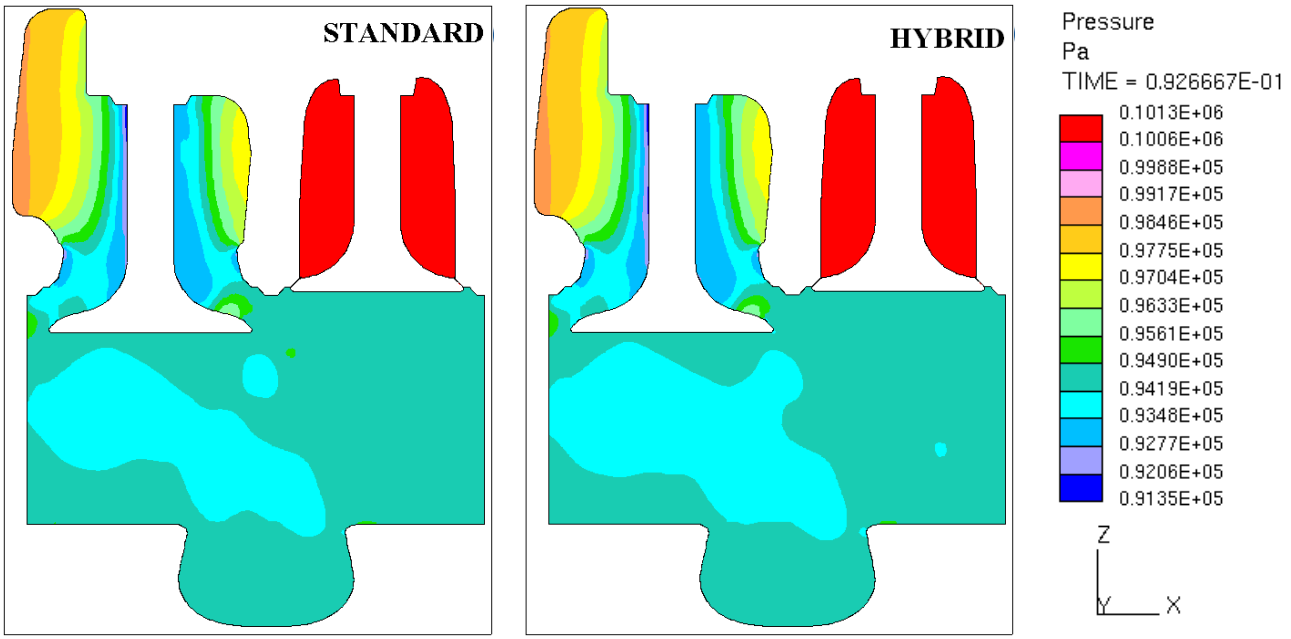

Figure 6. Pressure fields on section A-A, at 1154°

The Figure 8 shows the evolution along crank angle of the discharge coefficient and swirl ratio to the intake stroke. Also, it compares the hybrid and standard wall treatments. In the first stage of the evolution of discharge coefficient, a strong increase occurs after TDC (1080°), due to the opening of the intake valve, where in this moment the intake pressure port is higher than cylinder pressure. At 1095°, the discharge coefficient value reaches a local peak, and then decreases due to pressure equalization (port-cylinder). This brief decrease and a subsequent variation of the discharge coefficient can be attributed to the presence of dynamic effects and recirculations in the intake port.

At 1130°, according to the depression created inside the cylinder by downward piston movement, the cylinder pressure approaches its minimum value, and followed by intake valve open causes a significant increase in discharge coefficient, reaching its maximum value. After, there is a local reduction, due to corresponding increase in cylinder pressure ranging up to intake valve closing.

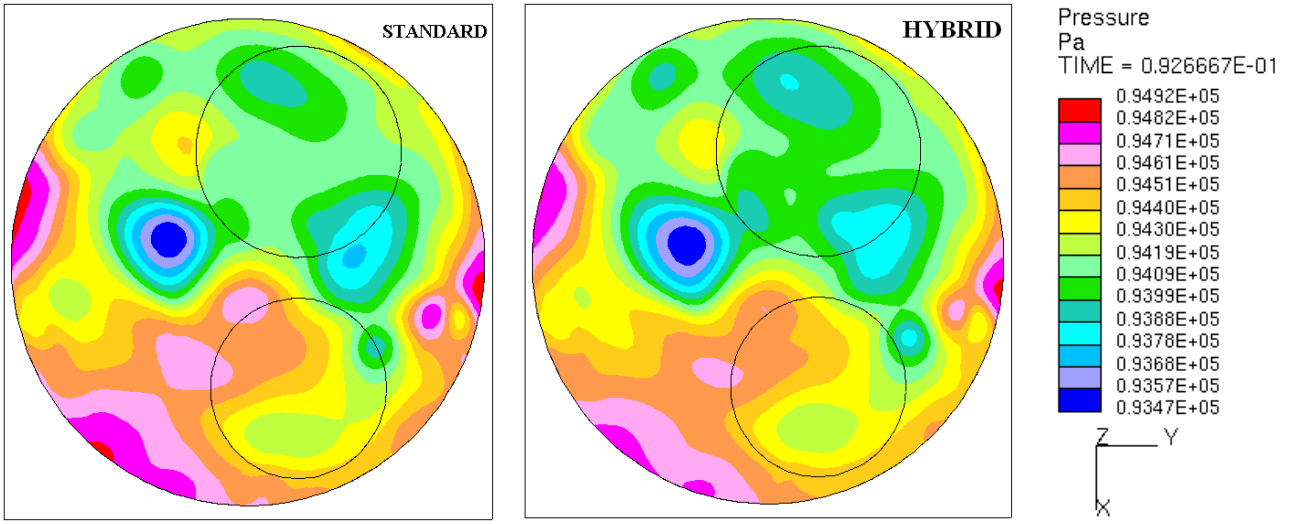

Figure 7. Pressure fields on section B-B, at 1154°

Regarding the swirl ratio, after TDC its value decreases reaching the minimum at 1095°. The negative value indicates that the resultant of the fluid rotation is clockwise. The swirl ratio reaches its maximum at 1206°, because the strong increase in the discharge coefficient and the considerable intake valve lift, where the counterclockwise flow predominates. The differences between the wall treatments are small.

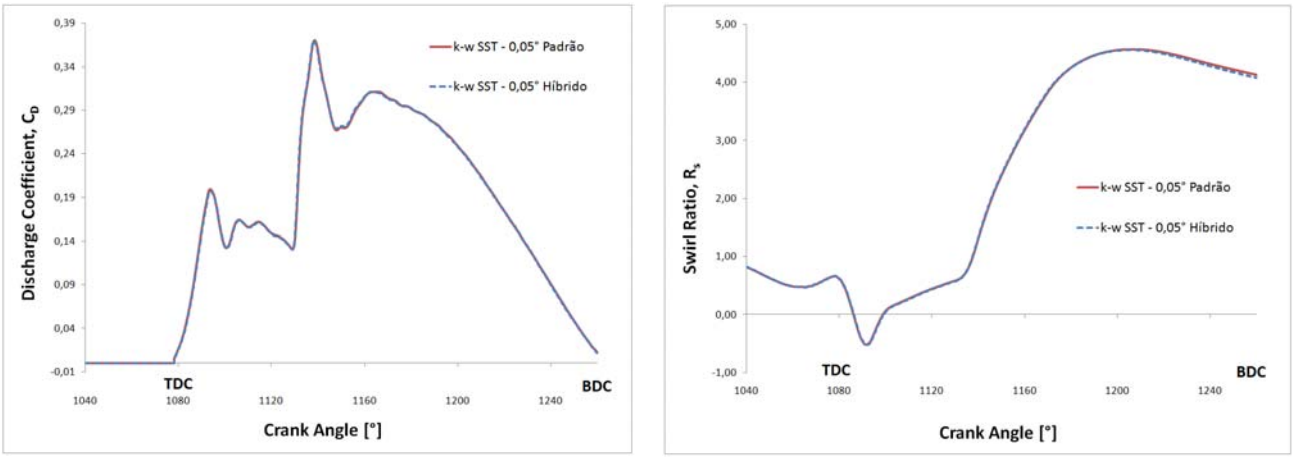

Figure 8. Evolution along crank angle of the discharge coefficient and swirl ratio

Other comparative parameters are presented in the Table 1. The relative differences between the wall treatments are small, for the air mass discharge and swirl ratio. Thus, the hybrid wall treatment is a good alternative to simulation the internal combustion engine flows.

Table 1. Comparative parameters at 1154°

Standard wall treatment		Hybrid wall treatment		Difference, relative to standard wall treatment[%]	
C_D	R_s	C_D	R_s	C_D	R_s
0.277406	2.723647	0.279590	2.739364	0.78	0.57

7. CONCLUSIONS

A three-dimensional unsteady turbulent compressible Navier-Stokes solver, Star-cd, was utilized in the present study to investigate the intake and in-cylinder flowfield of a two-valve direct injection compression ignition engine. The following conclusions were found:

- As expected, it is important that a high-quality complete grid be generated to resolve the transient flow processes found during intake stroke. It was very important to have a refined high-quality mesh with minimal skewness and non-uniformity, particularly at the intake port-cylinder interface.
- The comparative parameters presented in the Table 1, the discharge coefficient and swirl ratio, show that the difference relative to standard wall treatment is small for both parameters.
- Analyzing the observed differences between the flow patterns, it is possible to conclude that the presented deviations are not sufficient to prejudice a detailed project of the engine internal variable fields, necessary to a correct simulation of reactive flows (combustion).
- New searches need to be developed, aiming to clarify the simulation of the turbulence phenomenon in this kind of complex transient, multidimensional, compressible swirling non-isothermal flow, in movable domain.

8. ACKNOWLEDGEMENTS

The authors thank the financial support from CAPES, Brazil, through a master scholarship grant for Zancanaro, F.V.Jr., Falcão, C.E.G., and from CNPq, Brazil, through a doctoral grant to Andrade, G.S., and scientific productivity grant to Vielmo, H.A. Also, the authors would like to thank the CESUP, RS, Brazil.

9. REFERENCES

Baratta, M., Catania, A.E., Pesce, F.C., Spessa, E., Vielmo, H.A., 2008, "Numerical Analysis of a High Swirl-Generating Helical Intake Port for Diesel Engines". Proceedings of the 12th Brazilian Congress of Thermal Engineering and Sciences, Belo Horizonte, Brazil.

Baratta, M., Catania, A.E., Pesce, F.C., Spessa, E., Rech, C., Zancanaro, F.V.Jr, Vielmo, H.A., 2009, "Transient Numerical Analysis of a High Swirled Diesel Engine", 20th International Congress of Mechanical Engineering, Gramado – RS, Proceedings of COBEM, Rio de Janeiro, RJ: ABCM.

Bianchi, G.M., Cantore, G. and Fontanesi, S., 2002a, "Turbulence Modeling in CFD Simulation of ICE Intake Flows: The Discharge Coefficient Prediction", SAE Paper Nº 2002-01-1118.

Bianchi, G.M., Cantore, G., Parmeggiani, P., Michelassi, V., 2002b, "On Application of Nonlinear *k-ε* Models for Internal Combustion Engine Flows". Transactions of the ASME vol. 124, pp. 668-677.

Bianchi, G.M., Fontanesi, S., 2003, "On the Applications of Low-Reynolds Cubic *k-ε* Turbulence Models in 3D Simulations of ICE Intake Flows", SAE Paper Nº 2003-01-0003.

Ferrari, G., 2005, "Motori a Combustione Interna", Torino, Ed il Capitello, (in italian).

Fiat Research Center; Consiglio Nazionale delle Ricerche, 1982, "Motore Monocilindro Diesel con Distribuzione a 2 Valvole e Protezioni Termiche Camera di Combustione", Contract Nº 82.00047.93 (in italian).

Fiat Research Center; Consiglio Nazionale delle Ricerche, 1983, "Metodologia per la Caratterizzazione dei Condotti di Aspirazione Motori in Flusso Stazionario". Contract Nº 82.00047.93 (in italian).

Gosman, A.D., 1985, "Multidimensional Modeling of Cold Flows and Turbulence in Reciprocating Engine", SAE paper Nº. 850344.

Heywood, J.B., 1988, "Internal Combustion Engines", McGraw-Hill Inc.

Hinze, P.O., 1975, "Turbulence", 2nd Edition, McGraw-Hill, New York.

Hirsch, C., 2007, "Numerical Computational of Internal and External Flows – Vol. II: Computational Methods for Inviscid and Viscous Flows", John Wiley & Sons, New York.

Jones, W.P., 1980, "Prediction Methods for Turbulent Flow", Hemisphere, Washington, D.C., pp. 1-45.

Lakshminarayanan, P.A., Aghav, Y.V., 2010, "Modelling Diesel Combustion", Springer, Mechanical Engineering Serie.

Menter, F.R., 1993, "Zonal two Equation *k-ω* Turbulence Models for Aerodynamic Flows", Proc. 24th Fluid Dynamics Conf., Orlando, Florida, USA, Paper Nº. AIAA 93-2906.

Star-cd, 2008, "User Guides es-ice", CD-adapco.

Star-cd, 2009, "Methodology", CD-adapco.

Tindal, M.J., Williams, T.J., Aldoory, M., 1982, "The Effect of Inlet Port Design on Cylinder Gas motion in Direct Injection Diesel Engines", ASME, Flows in Internal Combustion Engines, pp. 101-111.

Warsi, Z.V.A., 1981, "Conservation Form of the Navier-Stokes Equations in General Nonsteady Coordinates", AIAA Journal, 19, pp. 240-242.

Wilkes, N.S. and Thompson, C.P., 1983, "An Evaluation of Higher-order Upwind Differencing for Elliptic Flow Problems", CSS 137, AERE, Harwell.

10. RESPONSIBILITY NOTICE

The authors are the only responsible for the printed material included in this paper.